JOURNAL OF Materials CHEMISTRY

Low temperature synthesis, structure and properties of $La_4BaCu_{5-x}M_xO_{13+\delta}$ (M = Ni, Co and Fe)†

C. Shivakumara,[a] M. S. Hegde,*[a] K. Sooryanarayana,[a] T. N. Guru Row[a] and G. N. Subbanna[b]

[a] *Solid State and Structural Chemistry Unit, and* [b] *Material Research Centre, Indian Institute of Science, Bangalore-560 012, India. E-mail: mshegde@sscu.iisc.ernet.in*

Received 8th June 1998, Accepted 9th September 1998

Oxygen deficient defect perovskite oxides having the general formula $La_4BaCu_{5-x}M_xO_{13+\delta}$ (M = Ni or Co, $0 \leqslant x \leqslant 1.0$, Fe, $x = 0.5$) have been synthesized from NaOH–KOH fluxes at 450 °C. Structures of these materials have been refined by the Rietveld method and confirmed by electron diffraction studies. Ni^{3+}, Co^{3+} and Fe^{3+} ions are shown to occupy the octahedral 1(a) site in the $La_4BaCu_5O_{13+\delta}$ structure. While the Ni substituted compound is metallic, composition controlled metal to insulator (M–I) like behaviour is observed for Co and Fe substituted compounds. While temperature independent magnetic susceptibility in the case of the Ni substituted compound indicated Pauli paramagnetic behaviour, Co and Fe substituted oxides were weakly paramagnetic.

Introduction

Among the new families of copper oxides discovered since the outbreak of superconductivity studies in 1986,[1] $La_4BaCu_5O_{13+\delta}$[2] is unique because it shows metallic behaviour down to lowest possible temperatures without undergoing a superconducting transition. $LaCuO_3$[3] is another oxide which shows metallic properties and no superconductivity. Otherwise, families of copper oxides such as $La_{2-x}Sr_xCuO_4$, $YBa_2Cu_3O_{7-\delta}$, and $Bi_2Sr_2Ca_{n-1}Cu_nO_{2n+4+\delta}$ ($n = 1$, 2, 3) *etc.*, show metallic and superconducting behaviour.[4–6] $La_4BaCu_5O_{13+\delta}$ crystallizes in a tetragonal structure in the space group $P4/m$, which is related to cubic perovskite subcell by $a \approx a_p\sqrt{5} = 8.65$ Å and $c = a_p = 3.86$ Å. The model structure[7] consists of groups of corner sharing CuO_5 pyramids linked through CuO_6 octahedra in such a way that each octahedron shares four corners with four pyramids and two corners with two octahedra and each pyramid is connected to four other pyramids and one octahedron. While substitution for the La site in this system has been performed by Vijayaraghavan *et al.*,[8] to the best of our knowledge, no substitution for Cu has been reported in the literature.

Superconducting oxides having the formula $La_{2-x}M_xCuO_4$(M = Na, K),[9] pyrochlore related oxides $A_2BB'O_7$ (A = La or Nd; BB′ = Pb, Sn or Bi)[10] and $RBa_2Cu_3O_{7-\delta}$ (R = Nd, Sm, Eu or Gd)[11] have been synthesized at low temperature by the NaOH–KOH flux method; however, $LaBa_2Cu_3O_{7-\delta}$ could not be synthesized by this method. It is known that partial substitution of Ni for Cu in $YBa_2Cu_3O_7$ occurs with Ni^{2+} occupying Cu(2) sites.[12] However, by partial substitution of Ni for Cu in $LaBa_2Cu_3O_7$, Ni^{3+} ions were shown to occupy the Cu(1) sites.[13] Also, $LaBa_2Cu_{3-x}Ni_xO_{7+\delta}$ ($x \leqslant 0.3$) showed metallic behaviour. In an attempt to synthesize the $LaBa_2Cu_3O_{7-\delta}$ phase by a low temperature route employing NaOH–KOH flux, we found that a thermodynamically stable $La_4BaCu_5O_{13+\delta}$ phase was obtained. In the $La_4BaCu_5O_{13+\delta}$ phase, out of five Cu, one Cu has octahedral coordination and since Ni^{3+}, Co^{3+} and Fe^{3+} ions prefer octahedral co-ordination, it was conceivable that one Cu can be substituted by these trivalent ions. Indeed we have synthesized $La_4BaCu_{5-x}M_xO_{13+\delta}$ (M = Co or Ni, $0 \leqslant x \leqslant 1$, Fe, $x \leqslant 0.5$) and here we report their low temperature synthesis, structure and properties.

Experimental

Stoichiometric amounts of high purity La_2O_3, CuO, NiO, Co_3O_4, $Fe(C_2O_4)\cdot 2H_2O$ and an excess of $Ba(OH)_2\cdot 8H_2O$ were ground in an agate mortar and added to a preheated 1 : 1 melt of NaOH and KOH (AR grade) at 400 °C in a recrystallized alumina crucible. A typical run contained La_2O_3 (1.3032 g), CuO (0.7954 g), $Ba(OH)_2\cdot 8H_2O$ (2.52 g), NaOH (10 g) and KOH (10 g) and led to a product $La_4BaCu_5O_{13.14}$. The temperature was increased and held at 450 °C for 2–4 days. Initially a clear blue solution was observed and gradually dark crystals precipitated. The melt was furnace cooled to room temperature, washed with distilled water followed by acetone and dried at 120 °C for 4 h. Powder X-ray diffraction patterns were recorded on a JEOL JDX-8P diffractometer, with a scan speed of 2° min^{-1} with a Cu-Kα ($\lambda = 1.5418$ Å; Ni filter) source to identify the phases. The structural parameters of some of these phases were refined by Rietveld profile analysis with the diffraction data collected on a STOE STADI/P diffractometer. The data were collected using a linear position sensitive detector (PSD) in the range of $5 < 2\theta/° < 80$ in steps of 0.02° in the transmission mode. The morphology and composition of these crystalline phases were obtained from scanning electron microscopy (SEM) and energy dispersive X-ray (EDX) analysis. Oxygen content was determined by iodometric titration and thermogravimetric analysis (TGA) by heating the sample under a stream of 15% H_2–85% Ar. Electron microscopy studies were carried out on as-synthesized samples to confirm the structure using a JEOL 200-CX transmission electron microscope. The polycrystalline powder was pelletised and sintered at 900 °C. No detectable change in the structure was observed in any of the samples. Further, a temperature programmed desorption (TPD) system attached to a VG QXK-300 quadrupole mass spectrometer showed no evolution of oxygen up to 750 °C indicating that there is no measurable change in the oxygen content after sintering. Further, oxygen estimation of the sample sintered at 750 °C and also at 900 °C were carried out and no measurable changes in the total oxygen content were observed. Electrical resistivity measurements were carried out on the sintered pellets by a four-probe method in the temperature range 300–15 K. dc Magnetic

†Contribution No. 1338 from Solid State and Structural Chemistry Unit.

susceptibility measurements have been performed in the range 300–20 K employing a Lewis coil force magnetometer (George Associates, Model 2000).

Results and discussion

Synthesis and structure

In an attempt to obtain the $LaBa_2Cu_2NiO_{7+\delta}$ phase by a low temperature method, stoichiometric amounts of La_2O_3, CuO and NiO with an excess of $Ba(OH)_2{\cdot}8H_2O$ were melted in an NaOH–KOH flux. The resulting crystalline material on examination by X-ray powder diffraction, electron microscopy and energy dispersive X-ray (EDX) analysis showed the presence of hexagonal $BaNiO_{2+\delta}$ and CuO, in addition to an unknown phase. Formation of $BaNiO_{2+\delta}$ in an alkali flux is known.[14] Therefore it was clear that almost all of the Ni in the melt formed a $BaNiO_{2+\delta}$ phase.

A composition corresponding to $LaBa_2Cu_3O_7$ was heated in the flux with the absence of Ni in the melt. The powder XRD data of the resulting product revealed the formation of the same unknown phase and CuO as an impurity. On careful examination of several crystals in spot mode by EDX, compositions of La : Ba : Cu was found to be 4 : 1 : 5 in the unknown phase indicating the possibility of $La_4BaCu_5O_{13+\delta}$ oxide formation. Then, the composition corresponding to $La_4BaCu_5O_{13+\delta}$ was heated in the flux and the powder X-ray diffraction pattern of this compound is shown in Fig. 1(a). All the lines could be indexed to the $La_4BaCu_5O_{13+\delta}$ phase. The lattice parameters agreed well with those reported in the literature.[7]

Mixed oxides $La_4BaCu_{5-x}Ni_xO_{13+\delta}$ ($0 \leqslant x \leqslant 1.0$) were then synthesized by taking stoichiometric amounts of La_2O_3, CuO and NiO with an excess of $Ba(OH)_2{\cdot}8H_2O$. An X-ray powder diffraction pattern for $x=1.0$ is shown in Fig. 1(b). As can be seen, all the lines could be indexed to the parent phase. In an attempt to substitute Ni to >1 atom per formula unit, compounds were prepared for composition $La_4BaCu_{4-x}Ni_{1+x}O_{13+\delta}$. However, the resulting products did not crystallize in the $La_4BaCu_5O_{13+\delta}$ structure.

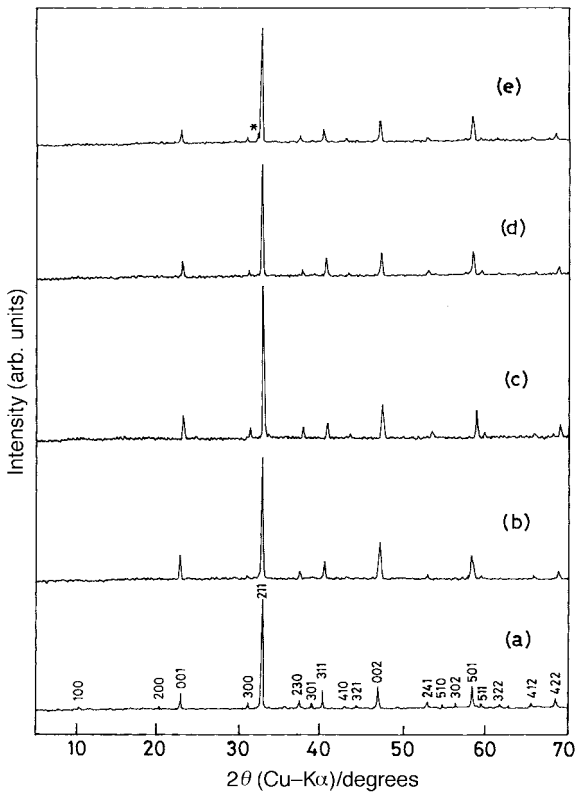

Fig. 1 Powder X-ray diffraction patterns of (a) $La_4BaCu_5O_{13.14}$ (b) $La_4BaCu_4NiO_{13.20}$, (c) $La_4BaCu_4CoO_{13.35}$, (d) $La_4BaCu_{4.5}Fe_{0.5}O_{13.28}$ and (e) $La_4BaCu_4FeO_{13+\delta}$ (asterisk indicates $LaFeO_3$ impurity phase).

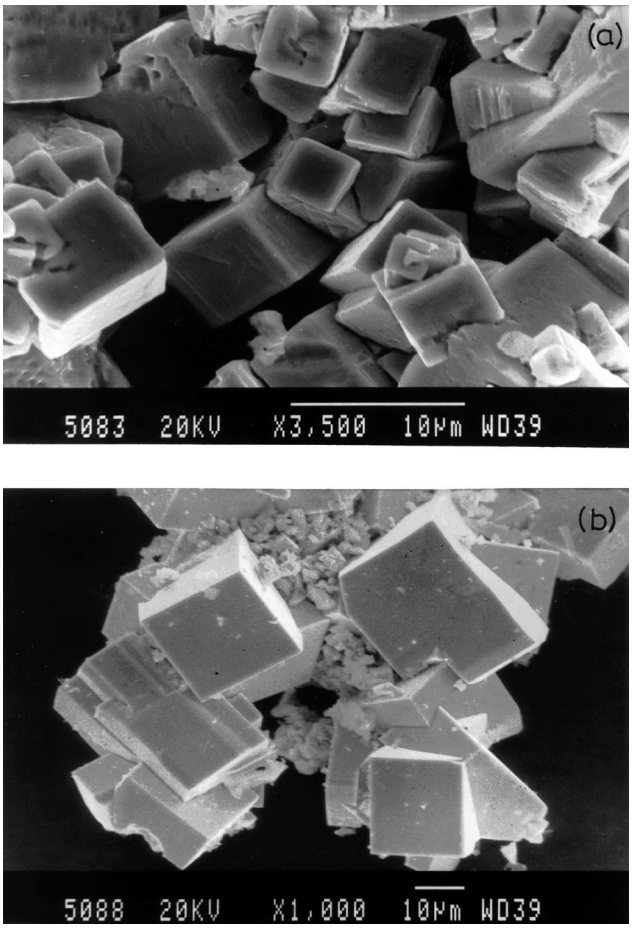

Fig. 2 Scanning electron micrographs of (a) $La_4BaCu_5O_{13.14}$ and (b) $La_4BaCu_4CoO_{13.35}$.

Mixed oxides $La_4BaCu_{5-x}Co_xO_{13+\delta}$ ($0 \leqslant x \leqslant 1$) were also synthesized and the pattern for $x=1$ is shown in Fig. 1(c). In the case of Fe, a value of x up to 0.5 could be substituted. For $x>0.5$, $LaFeO_3$ impurity phase was observed in the X-ray pattern in addition to Fe substituted $La_4BaCu_5O_{13+\delta}$. Diffraction patterns for $x=0.5$ and 1.0 are shown in Fig. 1(d) and (e), respectively.

Scanning electron micrographs of $La_4BaCu_5O_{13+\delta}$, and the Ni, Co and Fe substituted samples showed a cuboidal morphology. Crystals of size 0.1–0.2 mm were seen in these preparations. Typical scanning electron micrographs of the

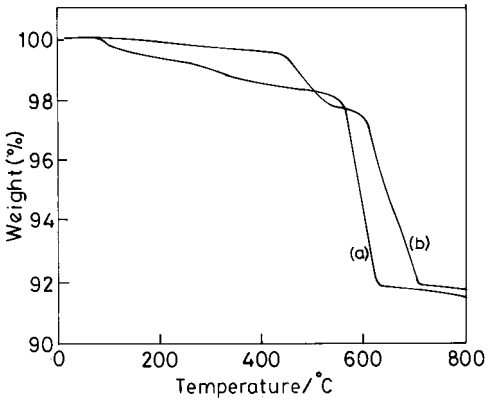

Fig. 3 Thermogravimetric analysis curves for (a) $La_4BaCu_5O_{13.14}$ and (b) $La_4BaCu_4CoO_{13.35}$.

Table 1 Compounds, lattice parameters and oxygen contents

Compound	Lattice parameter/Å		Oxygen content[a]	
	a	*c*	Iodometry[b]	TGA[c]
$La_4BaCu_5O_{13+\delta}$	8.668(3)	3.862(5)	13.14	13.23
$La_4BaCu_4NiO_{13+\delta}$	8.682(1)	3.869(6)	13.20	—
$La_4BaCu_4CoO_{13+\delta}$	8.679(1)	3.873(6)	13.35	13.29
$La_4BaCu_{4.5}Fe_{0.5}O_{13+\delta}$	8.673(3)	3.866(5)	13.28	13.25

[a]In atoms per formula unit. [b]Values accurate to within ± 0.02. [c]Values accurate to within ± 0.03.

parent and the Co substituted samples are shown in Fig. 2(a) and (b). EDX analysis in spot mode was performed on each of these samples. Results showed that the metal ions were within 3% of the formula corresponding to $La_4BaCu_4MO_{13+\delta}$ (M = Ni, Co) and $La_4BaCu_{4.5}Fe_{0.5}O_{13+\delta}$.

Thermogravimetric analysis curves for $La_4BaCu_5O_{13+\delta}$ and for the Co substituted sample are shown in Fig. 3. The TGA products contained La_2O_3, BaO and Cu as identified by X-ray diffraction. For Co and Ni substituted compounds, Cu, Co and Ni metal peaks could be detected in addition to La_2O_3 and BaO. Oxygen estimation was also determined by iodometric titration. Oxygen content as determined by thermogravimetric analysis as well as iodometric titration and the lattice parameters are summarized in Table 1.

Having confirmed the compositions of these phases, powder X-ray diffraction patterns were recorded for Rietveld analysis. Fig. 4 shows the observed, calculated and difference X-ray diffraction patterns for the $La_4BaCu_4CoO_{13.35}$ phase. Refinements were performed keeping Co in the octahedral site fully occupied and also allowing it to mix with the other allowed sites of copper. The refinements with Co in the octahedral site gave the best fit as indicated by the *R* factors given in Table 2. For $La_4BaCu_4NiO_{13.20}$ also, the structure was refined with Ni^{3+} in the 1(a) site similarly to the Co case and the final *R* factors are good. Mixing of Ni ions in Cu sites either fully or partially did not show any significant increase in *R* factors because of nearly similar scattering factors. Therefore, occupation of Ni^{3+} solely in the 1(a) position could not be ascertained. However, Ni^{3+} is known to prefer six co-ordination in perovskite related oxides such as $LaNiO_3$. It may be noted that $La_4BaCu_{4-x}Ni_{1+x}O_{13+\delta}$ does not crystallize in the parent structure. Therefore it is reasonable to expect Ni^{3+} ions to occupy the 1(a) position with six co-ordination while four Cu ions occupy 4(j) positions with five coordination. Details of the refinement with Ni in the 1(a) site are given in Table 2. Selected bond lengths for $La_4BaCu_4NiO_{13.20}$ and $La_4BaCu_4CoO_{13.35}$ are given in Table 3 and fractional

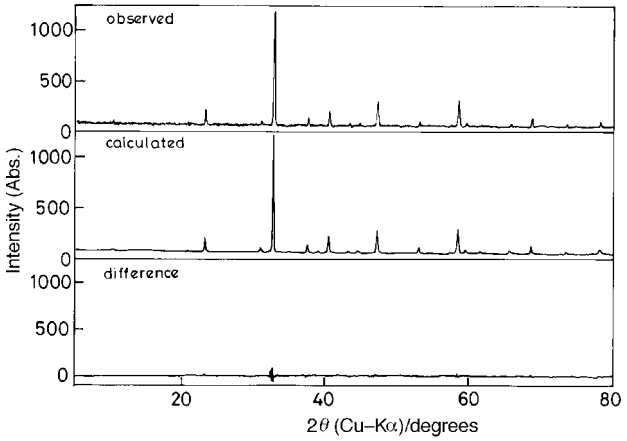

Fig. 4 Observed, calculated and difference powder X-ray patterns for $La_4BaCu_4CoO_{13.35}$.

Table 2 Crystallographic and structural refinement data for $La_4BaCu_4NiO_{13.20}$ and $La_4BaCu_4CoO_{13.35}$

Empirical formula	$La_4BaCu_4NiO_{13.20}$	$La_4BaCu_4CoO_{13.35}$
Crystal system	Tetragonal	Tetragonal
Space group	*P*4/*m*	*P*4/*m*
Unit cell dimensions/Å	$a = 8.6820(1)$	$a = 8.6790(1)$
	$c = 3.8699(6)$	$c = 3.8731(6)$
Volume/Å^3	291.69	291.72
Z	1.00	1.00
F(000)	533.8	532.6
D_c/g cm^{-3}	6.952	6.983
Radiation (λ/Å)	Cu-Kα_1 (1.540 56)	Cu-Kα_1 (1.540 56)
Diffractometer	STOE STADI/P	STOE STADI/P
Diffraction mode	Transmission	Transmission
Measurement method	2θ–ω	2θ–ω
$2\theta^\circ$ (begin, end, step)	5.0, 79.94, 0.02	5.0, 79.94, 0.02
2θ zero point	−0.1236	−0.1182
Absorption correction	Empirical	Empirical
Refinement method	Refinement F^2	Refinement F^2
Profile function	Pearson VII with exponent 2.00	Pearson VII with exponent 2.00
$R_{(1.\ hkl)}$	0.130	0.150
R_p	0.085	0.063
R_{wp}	0.108	0.080

Table 3 Selected bond lengths (Å) for $La_4BaCu_4NiO_{13.20}$ and $La_4BaCu_4CoO_{13.35}$

$La_4BaCu_4NiO_{13.20}$		$La_4BaCu_4CoO_{13.35}$	
Ni−O1 × 2	1.935(3)	Co−O1 × 2	1.937(3)
Ni−O4 × 4	1.932(33)	Co−O4 × 4	1.973(23)
Cu−O2 × 1	1.721(41)	Cu−O2 × 1	1.707(44)
Cu−O3 × 1	2.156(20)	Cu−O3 × 1	2.235(19)
Cu−O3′ × 1	2.076(10)	Cu−O3′ × 1	1.931(20)
Cu−O4 × 1	1.833(23)	Cu−O4 × 1	1.870(23)
Cu−O5 × 2	1.951(25)	Cu−O5 × 2	1.944(20)
Ba−O3 × 8	2.844(15)	Ba−O3 × 8	2.861(15)
Ba−O5 × 4	2.903(16)	Ba−O5 × 4	3.056(20)
La−O1 × 1	2.670(20)	La−O1 × 1	2.643(18)
La−O2 × 2	2.905(16)	La−O2 × 2	2.940(18)
La−O3 × 2	2.582(13)	La−O3 × 2	2.576(13)
La−O4 × 2	2.749(14)	La−O4 × 2	2.671(18)
La−O4′ × 2	2.659(13)	La−O4′ × 2	2.717(16)
La−O5 × 1	2.859(17)	La−O5 × 1	2.758(20)
La−O5′ × 1	2.565(19)	La−O5′ × 1	2.738(20)
La−O5″ × 1	2.808(19)	La−O5″ × 1	2.648(20)

Table 4 Fractional atomic coordinates and isotropic thermal parameters (Å^2) for $La_4BaCu_4NiO_{13.20}$ and $La_4BaCu_4CoO_{13.35}$

$La_4BaCu_4NiO_{13.20}$

Atom	*x*	*y*	*z*	U_{iso}
La	0.1221(22)	0.2823(27)	0.50000	0.020(14)
Ba	0.50000	0.50000	0.50000	0.030(1)
Ni	0.00000	0.00000	0.00000	0.022(6)
Cu	0.3988(50)	0.1705(38)	0.00000	0.022(6)
O1	0.00000	0.00000	0.50000	0.05000
O2	0.00000	0.50000	0.00000	0.05000
O3	0.2858(251)	0.3917(205)	0.00000	0.05000
O4	0.2041(279)	0.0888(224)	0.00000	0.05000
O5	0.4268(230)	0.1738(189)	0.50000	0.05000

$La_4BaCu_4CoO_{13.35}$

Atom	*x*	*y*	*z*	U_{iso}
La	0.1248(25)	0.2778(28)	0.50000	0.018(4)
Ba	0.50000	0.50000	0.50000	0.050(2)
Cu	0.4073(52)	0.1735(51)	0.00000	0.018(8)
Co	0.00000	0.00000	0.00000	0.018(8)
O1	0.00000	0.00000	0.50000	0.05000
O2	0.00000	0.50000	0.00000	0.05000
O3	0.2801(242)	0.3974(196)	0.00000	0.05000
O4	0.2111(262)	0.0843(311)	0.00000	0.05000
O5	0.4188(236)	0.1574(219)	0.50000	0.05000

atomic coordinates and isotropic thermal parameters are given in Table 4.

Full Crystallographic details, excluding structure factors, have been deposited at the Cambridge Crystallographic Data Centre (CCDC). See Information for Authors, *J. Mater. Chem.*, 1998, Issue 1. Any request to the CCDC for this material should quote the full literature citation and the reference number 1145/117.

Selected area electron diffraction patterns were recorded on several crystallites, to confirm the formation of the $La_4BaCu_5O_{13.14}$ phase. Fig. 5(a) and (b) show the electron diffraction patterns of the parent phase recorded along (001) and (010) zone axes. Lattice parameters obtained here agree well with the X-ray results and those reported in the literature.[7] The electron diffraction pattern of the Ni substituted oxide $La_4BaCu_4NiO_{13.20}$ is shown in Fig. 5(c) recorded along the (001) zone axis. High resolution images were also recorded on the parent as well as Ni and Co substituted oxides. Fig. 5(d) shows the high resolution image recorded along (010) for the Co substituted oxide. Observed lattice fringes of *ca.* 8.65 Å correspond to the '*a*' parameter of the unit cell. The inset shows the corresponding diffraction pattern. Thus, electron microscopic studies confirm the formation of $La_4BaCu_5O_{13+\delta}$, and the Ni and Co substituted phases by our low temperature route.

Synthesis of these oxides using a low temperature NaOH–KOH flux is important, because, Ni, Co and Fe substituted compounds cannot be synthesized by a solid state route. Substitution of both Co and Ni up to one atom per formula unit has been achieved.

Electrical and magnetic properties

Fig. 6(a) shows plots of electrical resistivity *vs.* temperature between 300 and 15 K for $La_4BaCu_5O_{13.14}$, $La_4BaCu_4NiO_{13.20}$ and $La_4BaCu_4CoO_{13.35}$. The parent and the Ni substituted phases showed metallic behaviour. $La_4BaCu_{5-x}Ni_xO_{13+\delta}$ ($x=$ 0.25, 0.50) were also synthesized and these compounds also showed metallic behaviour, while the $La_4BaCu_4CoO_{13.35}$ oxide showed semiconducting like behaviour. It is important to note

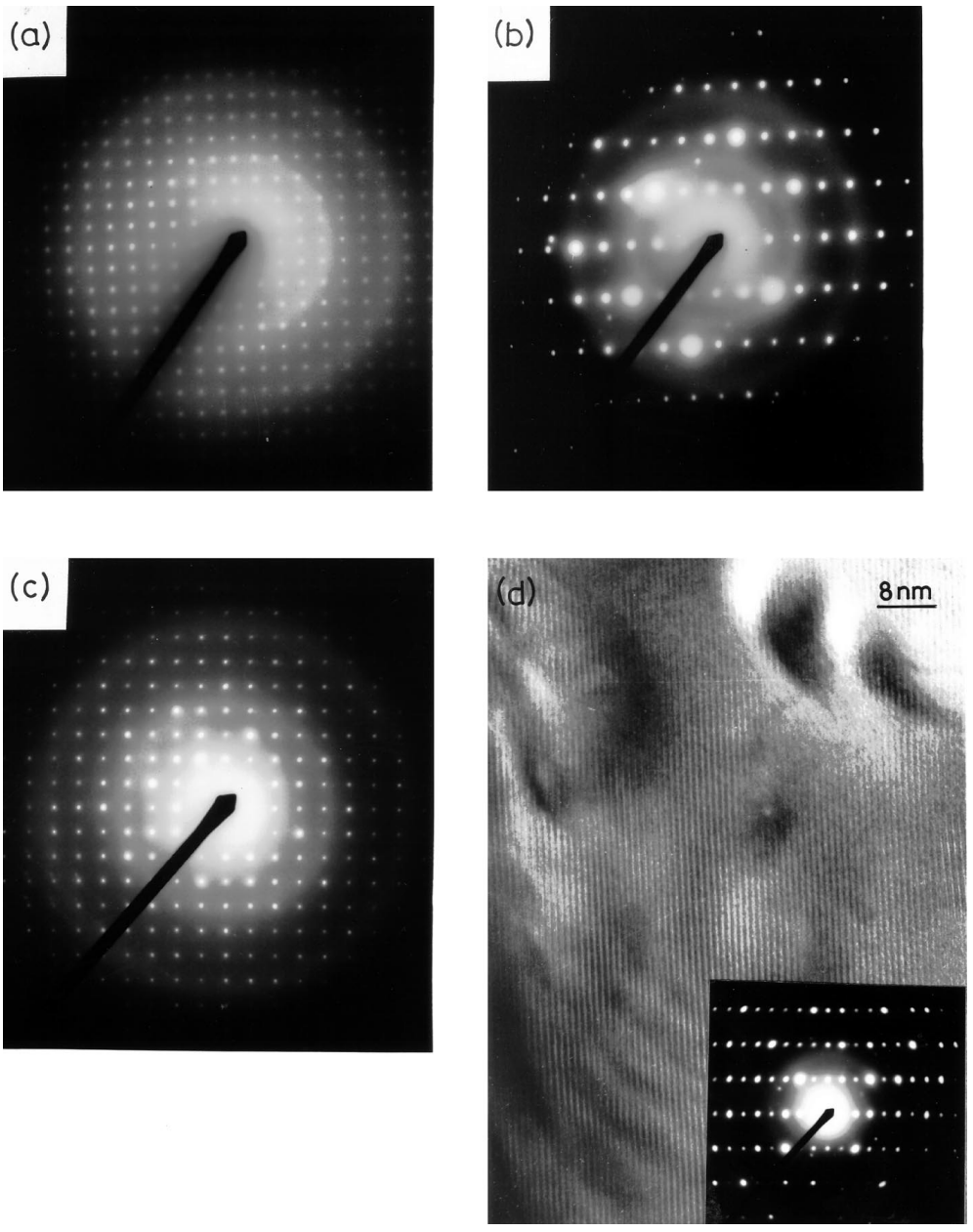

Fig. 5 Selected area electron diffraction patterns of $La_4BaCu_5O_{13.14}$ in (a) (001) and (b) (010) zone axes; SAED of $La_4BaCu_4NiO_{13.20}$ in (c) (001) zone axis and (d) high resolution image of $La_4BaCu_4CoO_{13.35}$ showing *ca.* 8.65 Å periodicity; inset shows corresponding diffraction pattern recorded along the (010) axis.

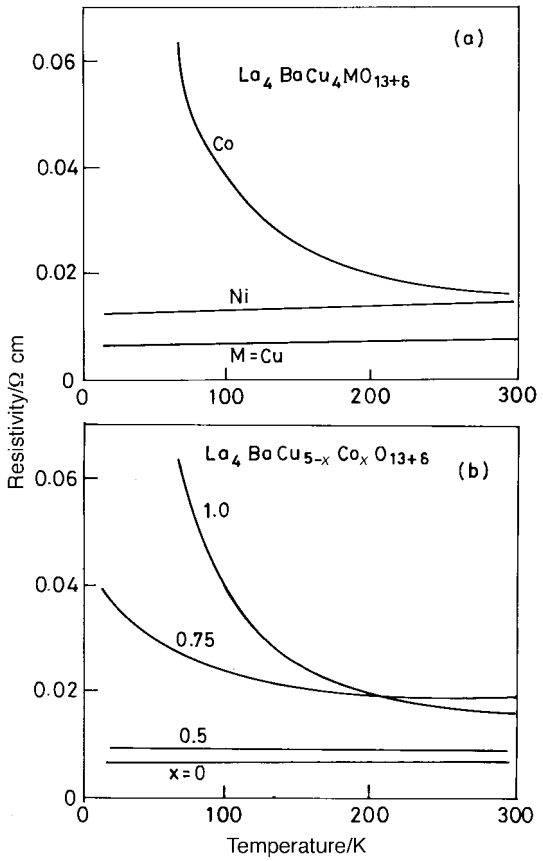

Fig. 6 Resistivity as a function of temperature curves for (a) $La_4BaCu_{5-x}M_xO_{13+\delta}$ and (b) $La_4BaCu_{5-x}Co_xO_{13+\delta}$.

that the resistivity of $La_4BaCu_4CoO_{13.35}$ at 300 K is of the same order of magnitude as that of the parent as well as the Ni substituted oxides. Fig. 6(b) shows resistivity *vs.* temperature plots of $La_4BaCu_{5-x}Co_xO_{13+\delta}$ ($0 \leqslant x \leqslant 1.0$). For $x=0.5$, the compound is still metallic and for $x>0.5$, semiconducting like behaviour is observed. Thus, the Co doped oxide shows composition controlled metal to insulating like behaviour as the cobalt content increased from 0 to 1.

Magnetic susceptibility *vs.* temperature plots of $La_4BaCu_5O_{13.14}$, $La_4BaCu_4NiO_{13.20}$, $La_4BaCu_{4.5}Co_{0.5}O_{13+\delta}$ and $La_4BaCu_4CoO_{13.35}$ are shown in Fig. 7. Both Cu and Ni phases showed temperature independent susceptibility from 300 to 20 K.

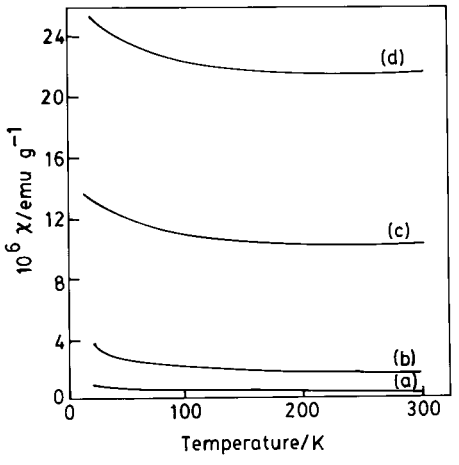

Fig. 7 Magnetic susceptibility as a function of temperature curves for (a) $La_4BaCu_5O_{13.14}$, (b) $La_4BaCu_4NiO_{13.20}$, (c) $La_4BaCu_{4.5}Co_{0.5}O_{13+\delta}$ and (d) $La_4BaCu_4CoO_{13.35}$.

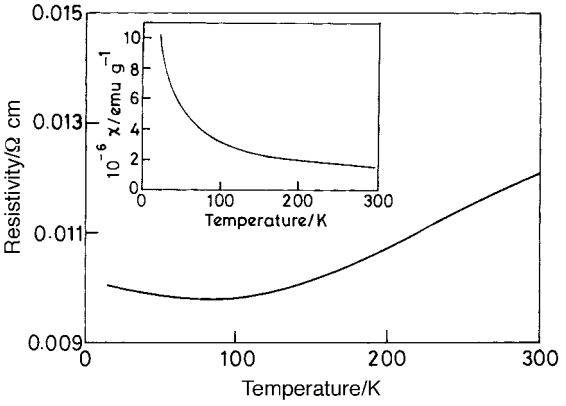

Fig. 8 Resistivity *vs.* temperature curve for $La_4BaCu_{4.5}Fe_{0.5}O_{13.28}$. In inset susceptibility *vs.* temperature plot is given.

The susceptibility value of the Co containing phase was higher at 300 K and nearly temperature independent and weak paramagnetic like behaviour was observed as the sample is cooled which did not follow the Curie law. As the Co content was increased, the susceptibility at 300 K increased from 3×10^{-6} to 18×10^{-6} emu g^{-1} from $x=0$ to 1.0. The susceptibility χ was fitted to a function $(C/T)+\alpha$, where α is a temperature independent contribution. For $La_4BaCu_{5-x}Co_xO_{13+\delta}$, magnetic moments were 0.3, 0.8 and 1.0 μ_B for $x=0$, 0.5 and 1.0, respectively, per formula unit. The low value of 0.06 μ_B per Cu is characteristic of delocalized carriers.[2] If Co^{3+} ions in this compound are in high spin state, the expected moment is 4.7 μ_B, even assuming that the magnetic moment solely arises from Co in $La_4BaCu_4CoO_{13.35}$. The low value of 1.0 μ_B observed here suggests that the spins on Co are not fully localized.

Fig. 8 shows the resistivity *vs.* temperature plot of $La_4BaCu_{4.5}Fe_{0.5}O_{13.28}$. The oxide showed metallic behaviour from 300 to 100 K and started showing semiconducting like behaviour below 100 K. In the inset the susceptibility as a function of temperature is shown. The results reveal that the Fe doped compound exhibits weakly paramagnetic behaviour.

Metallic behaviour in $La_4BaCu_5O_{13.14}$ is due to complete overlap of Cu 3d and O 2p bands. The average oxidation state of Cu in this compound is 2.45. This can be represented by the equilibrium:[15]

$$Cu^{3+}+O^{2-} \rightleftharpoons Cu^{2+}+O^{1-} \quad (1)$$

This indicates the presence of holes on copper as well as oxygen. The Ni, Co and Fe substituted oxides are made under highly oxidizing conditions and these metal ions should be in the +3 state. This follows from the fact that $LaNiO_3$, $LaCoO_3$ and $LaFeO_3$ can be synthesized from NaOH–KOH flux at 450 °C. Thus, with Ni^{3+} in $La_4BaCu_4NiO_{13.2}$, the average oxidation number of Cu is 2.35. Accordingly, the hole concentration on Cu is high as indicated by equilibrium (1). As in $LaNiO_3$, Ni^{3+} in this compound is in octahedral coordination. Since $LaNiO_3$ itself is a metallic and Pauli paramagnetic oxide, metallic and Pauli paramagnetic behaviour is expected for $La_4BaCu_4NiO_{13.2}$. A similar situation exists in $LaBa_2Cu_{3-x}Ni_xO_{7+\delta}$ ($0.1 \leqslant x \leqslant 0.3$),[13] where Ni occupies the Cu(1) sites in the +3 state and the compounds are metallic down to 15 K.

The cobalt substituted compound, $La_4BaCu_4CoO_{13.35}$, shows semiconducting behaviour. Assuming Co in the +3 oxidation state, the average oxidation state of Cu is 2.42. Therefore, equilibrium (1) should exist in this compound. Since, oxidation of Co^{3+} to Co^{4+} is more facile than Cu^{2+} to Cu^{3+}, it is possible to consider additional electron exchange *via* oxygen as follows:

$$Cu^{3+}+Co^{3+} \rightleftharpoons Cu^{2+}+Co^{4+} \quad (2)$$

A similar situation exists in $LaBa_2Cu_2CoO_{7.35}$ which also shows semiconducting behaviour.[16] It should be noted that $LaCoO_3$ is semiconducting and the presence of Co^{3+} or excess of Cu^{2+} by equilibrium (2) would lead to a semiconducting behaviour in this compound. A fairly high conductivity at 300 K in $La_4BaCu_4CoO_{13.35}$ can be attributed to the high oxidation number of Cu (2.42) or equivalently, high concentration of holes.

For the Fe substituted oxide, even at $x=0.5$, the compound exhibits semiconducting behaviour below 100 K. Here also,

$$Cu^{3+} + Fe^{3+} \rightleftharpoons Cu^{2+} + Fe^{4+} \quad (3)$$

equilibrium can occur as is seen in $La_{2-x}Sr_xCu_{1-y}Fe_yO_4$.[17] Unlike in the case of divalent ion doped $LaCoO_3$ (*e.g.* $La_{0.67}Sr_{0.33}CoO_3$) which is metallic, $La_{1-x}Sr_xFeO_3$ phases do not show metallic behaviour. Therefore, semiconducting behaviour is expected for the Fe substituted compound even for $x=0.5$.

Conclusions

$La_4BaCu_5O_{13.14}$ and Ni, Co and Fe substituted phases have been synthesized by a low temperature route employing an NaOH–KOH flux. While the parent $La_4BaCu_5O_{13.14}$ and the $La_4BaCu_4NiO_{13.20}$ showed metallic and Pauli paramagnetic behaviour, Co and Fe substituted oxides show composition controlled metal to insulator transitions and they are weakly paramagnetic. These observations are explained by possible charge exchange between Co^{3+} and Fe^{3+} with Cu^{3+} *via* oxide ion.

We thank Professor J. Gopalakrishnan for useful suggestions and the Department of Science and Technology for financial assistance. One of us (KS) thanks the Council of Scientific and Industrial Research (CSIR) for a senior research fellowship.

References

1 J. G. Bednorz and K. A. Muller, *Z. Phys. B*, 1986, **64**, 189.
2 C. Michel, L. Er-Rakho and B. Raveau, *Mater. Res. Bull.*, 1985, **20**, 667.
3 G. Demazeau, C. Parent, M. Pouchard and P. Hagenmuller, *Mater. Res. Bull.*, 1972, **7**, 913: J. B.Goodenough, N. F. Mott, M. Pouchard, G. Demazeau and P. Hagenmuller, *Mater. Res. Bull.*, 1973, **8**, 647.
4 R. J. Cava, R. B. Van Dover, B. Batlogg and E. A. Rietman, *Phys. Rev. Lett.*, 1987, **58**, 408.
5 M. K. Wu, J. R. Ashburn, C. J. Torng, P. H. Hor, R. L. Meng, L. Gao, Z. J. Huang, Y. Q. Wang and C. W. Chu, *Phys. Rev. Lett*., 1987, **58**, 908.
6 M. Maeda, Y. Tanaka, M. Fukutomi and A. Asano, *Jpn. J. Appl. Phys*., 1988, **27**, L209.
7 C. Michel, L. Er-Rakho, M. Herview, J. Pannetier and B. Raveau, *J. Solid State Chem*., 1987, **68**, 143.
8 R. Vijayaraghavan, R. A. Mohan Ram and C. N. R. Rao, *J. Solid State Chem*., 1988, **78**, 316.
9 W. K. Ham, G. F. Holland and A. M. Stacy, *J. Am. Chem. Soc.*, 1988, **110**, 5214.
10 S. Uma and J. Gopalakrishnan, *J. Solid State Chem.*, 1993, **105**, 595.
11 L. N. Marquez, S. W. Keller and A. M. Stacy, *Chem. Mater*., 1993, **5**, 761.
12 J. M. Tarascon, P. Barboux, P. F. Miceli, L. H. Greene, G. W. Hull, M. Eibshutz and S. A. Sunshine, *Phys. Rev. B*, 1998, **37**, 7458.
13 S. Sundar Manoharan, S. Ramesh, M. S. Hegde and G. N. Subbanna, *J. Solid State Chem.*, 1994, **112**, 281.
14 J. DiCarlo, I. Yazdi, and A. J. Jacobson, *J. Solid State Chem*., 1994, **109**, 223.
15 J. B. Goodenough and A. Manthiram, *J. Solid State Chem*., 1990, **88**, 115.
16 S. Ramesh, N. Y. Vasanthacharya, M. S. Hegde, G. N. Subbanna, H. Rajagopal, A . Sequiera and S. K. Paranjpe, *Physica C*, 1995, **253**, 243; S. Ramesh and M. S. Hegde, *J. Phys. Chem.*, 1996, **100**, 8443.
17 K. Ramesha, S. Uma, N. Y. Vasanthacharya and J. Gopalakrishnan, *J. Solid State Chem.*, 1997, **128**, 169.

Paper 8/04334E